Separation Science and Technology
Publication details, including instructions for authors and subscription information:
http://www.informaworld.com/smpp/title~content=t713708471

OIL/WATER SEPARATION USING NANOFILTRATION MEMBRANE TECHNOLOGY

Eugene Park[a]; Stanley M. Barnett[a]
[a] Chemical Engineering Department, University of Rhode Island, Center for Pollution Prevention, Kingston, Rhode Island, U.S.A.

Online publication date: 31 May 2001

To cite this Article Park, Eugene and Barnett, Stanley M.(2001) 'OIL/WATER SEPARATION USING NANOFILTRATION MEMBRANE TECHNOLOGY', Separation Science and Technology, 36: 7, 1527 — 1542
To link to this Article: DOI: 10.1081/SS-100103886
URL: http://dx.doi.org/10.1081/SS-100103886

SEPARATION SCIENCE AND TECHNOLOGY, 36(7), 1527–1542 (2001)

OIL/WATER SEPARATION USING NANOFILTRATION MEMBRANE TECHNOLOGY

Eugene Park and Stanley M. Barnett*

University of Rhode Island,
Center for Pollution Prevention,
Chemical Engineering Department,
Kingston, Rhode Island 02881-0805

ABSTRACT

Traditionally, ultrafiltration has been used to separate relatively clean water from oil/water emulsions. This water was once suitable for discharge to all sewer lines, but in general, it was inadequate for reuse. Recent changes in sewer discharge limits have created a need to generate cleaner water. A different type of membrane filtration, nanofiltration, may offer an effective means of recycling water from oil solutions or for generating clean enough water for discharge.

Results of ultrafiltration and nanofiltration batch concentration tests indicate that nanofiltration can effectively treat industrial machining coolant. The mass transfer model fit the flux behavior. At lower pressures, nanofiltration flux was slightly lower, mostly due to the higher membrane resistance of the nanofilter. However, at higher operating pressures, the nanofiltration mass transfer coefficient *increased* while the ultrafiltration transfer coefficient *de-*

*Corresponding author.

creased. Except at very high percent recovery levels, lower levels of COD and conductivity were observed in the nanofilter permeate as compared to the ultrafilter permeate; the quality of nanofiltration permeate resembled that of ultrafiltration permeate near the end of the concentration cycle.

INTRODUCTION

Oil-in-water emulsions are common by-products of many types of manufacturing operations, such as the machining and washing of metal parts. Many of these solutions contain over 90% water. The oil is chemically emulsified into the water phase because of the presence of surfactants. The entire mixture, even though it contains less than 10% total oil, cannot be discharged. In addition, metals may be present in the fluid. In most localities, this waste fluid must be shipped off-site as hazardous waste. Membrane filtration can be used to remove most of the water from the emulsion and therefore reduce the volume of oil-containing solutions.

Traditional ultrafiltration technology has provided for relatively clean water that was once suitable for sewer discharge but generally inadequate for reuse. However, recent changes in sewer discharge limits (oil and grease, COD, metals, etc.) have created a need to generate even cleaner water, with an emphasis on reuse. In many locations, ultrafiltration treatment alone does not meet discharge laws. Some companies have resorted to secondary treatment steps in order to comply with the tightening regulations. A related type of membrane technology, nanofiltration (NF), may offer a cost-effective means of separating recyclable or sewerable water from oil. The feasibility of nanofiltration is explored in this paper.

Nanofiltration, otherwise known as "loose reverse osmosis," operates as a water softener rather than as a complete purifier (1). Compared with true reverse osmosis (RO), NF exhibits salt and metal ion rejection percentages that are typically lower (50–80% vs. 99+%), and organic molecule rejection characteristics that are somewhat poorer (500 vs. 100 molecular weight) (2). In comparison, ultrafiltration (UF) membranes allow almost all soluble material to pass except for large proteins (>10,000 molecular weight) (3); the NF membrane has much smaller pores and is thus able to significantly reject many of the smaller organics that pass through the UF membrane. As a result, nanofiltration can be classified between RO and UF on the filtration spectrum.

NF has a very strong potential to serve in waste recovery applications like oil/water separation. The NF permeate from oily solutions is cleaner than the UF permeate, therefore allowing more opportunity for in-house recycle. If discharge is preferred, NF permeate can also be clean enough to meet tightening discharge requirements.

The membrane structure is not considered a perfect barrier. Both the ultrafiltration and nanofiltration membranes that were tested in this study are of the thin film composite type, in which a thin polymeric layer is coated over a more porous support base. A distribution of pore sizes exists in the thin layer where the average ultrafiltration pore size is much larger than that of the nanofiltration membrane. The membranes tested were oleophobic (oil-rejecting) due to the surface properties of the material.

Because of the convective transport of solute to the membrane surface, a phenomenon called *concentration polarization* results (4). Once enough solute is brought to the membrane surface, a gel layer forms. One important parameter that affects the short- and long-term influences of concentration polarization on permeate flux is the apparent tangential velocity (v) or Reynolds number. At a particular operating pressure, if v is not high enough, the gel layer that forms at the membrane surface can thicken and can become almost irreversibly attached to the membrane surface, a phenomenon called *fouling* (5). Only extreme cleaning methods like high pH or high temperature, conditions that most polymeric membranes cannot withstand, can remove the foulants. In addition, too much applied pressure can actually compact the gel layer and further facilitate fouling (6). As a result, the influence of concentration polarization should be minimized. One theoretical model is based on concentration polarization: the mass transfer (film theory) model.

Mass Transfer Model

A result of concentration polarization is the significant deviation of permeate flux from pure solvent flux. As the applied pressure increases and the flux vs. pressure curve flattens out to become more independent of pressure, a gel layer of solute forms. Solute particles are brought to the membrane surface through convective transport of the solvent flow, creating concentration polarization. As the pressure is increased and more solute is forced against the membrane barrier, a gel layer eventually forms. In the mass transfer model, this gel layer concentration is assumed constant, independent of operating conditions (5). Because of the concentration gradient, back diffusion of the solute also occurs. At a steady state, the opposite movements of solute balance each other and integrate over the mass transfer boundary layer thickness, resulting in

$$J = k \times \ln(C_m/C_b) \tag{1}$$

where J is the solvent or permeate flow rate, k is the mass transfer coefficient, C_m is the concentration of solute at the membrane surface, and C_b is the solute concentration away from the membrane (bulk concentration). Since a gel layer is assumed, C_m can be written as C_g, a constant for a particular solution. Equation (1) depicts the influence of solute concentration on flux. As the bulk solution becomes

MARCEL DEKKER, INC.
270 Madison Avenue, New York, New York 10016

concentrated, permeate flux drops. Theoretically, when C_b approaches C_g, the flux becomes zero.

The mass transfer coefficient, k, can be determined by a variety of transport properties, including diffusivity and turbulence. If the feed flow is turbulent, the following correlation is used (7):

$$Sh = 0.023 Re^{0.8} Sc^{0.33} \tag{2}$$

where

Sh = Sherwood # = kd_h/D
Re = Reynolds # = kd_h/v
Sc = Schmidt # = v/D
d_h = equivalent hydraulic diameter
v = average tangential velocity of fluid
v = kinematic viscosity of fluid

then

$$k = 0.023(v^{0.8} D^{0.67})/(d_h \cdot 2^{0.47}) \tag{3}$$

For a given solution and membrane process, v (feed velocity or tangential velocity) is the only parameter that can be varied to affect the mass transfer coefficient, k.

PROCEDURE

All membrane tests were carried out in a batch, recirculating mode (see Fig. 1). For each run, the starting batch volume was 150 l. Both pressure and

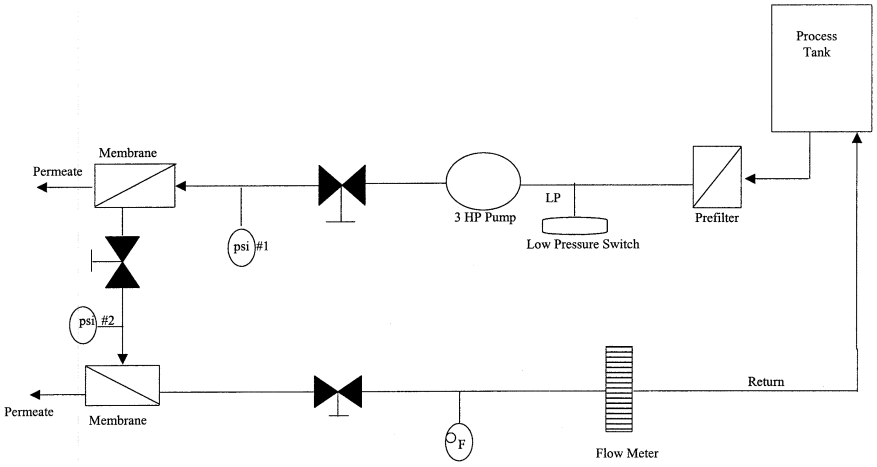

Figure 1. Process schematic.

MARCEL DEKKER, INC.
270 Madison Avenue, New York, New York 10016

feed flow (velocity) could be varied. A cooling coil heat exchanger was used to minimize temperature variance. Average transmembrane pressures ranged from 413 kPa to 1206 kPa. The average transmembrane pressure readings were taken from pressure gauge #2 (Fig. 1), which was situated between the two membrane modules. The membrane module configuration was spiral. For each run, two membrane modules containing the same type of membrane were used in series, providing a total available membrane area of 1.6 m^2. Feed flows were varied from 21 liters per minute (lpm) to 32 lpm, which correlate to apparent linear velocities of 0.2 to 0.33 m/sec. The apparent linear velocity, v, was calculated assuming smooth channels; in reality, the spacer channels in the membrane module are of irregular geometry to produce artificial turbulence. Feed flow was actually measured as concentrate flow; since the permeate flow was less than 1% of the total feed flow, the concentrate flow would always be at least 99% of the true feed flow. One type of ultrafilter and one type of nanofilter membrane, both manufactured by Desalination Systems (Escondido, CA), were compared. The ultrafiltration membrane was model G-50, and the nanofiltration membrane was model DS-5. Previous research indicates that the G-50 membrane exhibits a molecular weight cut-off of ~15,000 using glycol-based standards, and that the DS-5 membrane rejects 200–500 molecular weight organic species (2,3). Partial rejection of ions also has been noted as process characteristics of the DS-5 membrane.

The oil/water emulsion tested was a water-soluble machining coolant (International Compound #1678, made by International Chemical Co.) commonly used in industry. The coolant contained low levels of dissolved solids and hence exhibited low osmotic pressure. The test sample was made from new coolant concentrate by mixing four parts water to one part concentrate. An acid split test on the mixed solution revealed a mineral oil concentration of 15% v/v. A conductivity measurement indicated around 1200 μmho. The average of three COD analyses of the feed solution was 185,000 mg/liter. The pH of the coolant mixture was 9. Since the emulsified solution contained a multitude of organic constituents (proprietary), the COD measurement provided an overall reading of the total organic levels.

It is known that machining coolants in general contain mineral oil, surfactants, rust inhibitors, biocides, and defoaming agents. The conductivity readings provide an indirect measurement of total dissolved solids (TDS), a critical parameter that affects osmotic pressure and is also another measure of the permeate quality. While many other studies have focused on specific chemical species (e.g., protein separation), this research dealt with much more complicated chemical mixtures; for practical reasons, then, the more non-specific analytical techniques were used to analyze the solutions.

Batch runs were 150 l for each test. Permeate samples were taken throughout each run for flow measurement and later analyzed for pH, COD, and conductivity. Despite the use of the cooling coil, solution temperature increased during

MARCEL DEKKER, INC.
270 Madison Avenue, New York, New York 10016

Table 1. Coolant Test Runs

Run #	Membrane	Ave. Press. (kPa)	Appar. Lin. Vel. (m/sec)
1	Ultrafilter	413	0.21
2	Ultrafilter	413	0.27
3	Ultrafilter	413	0.34
4	Ultrafilter	689	0.21
5	Ultrafilter	689	0.27
6	Ultrafilter	689	0.34
7	Ultrafilter	965	0.21
8	Ultrafilter	965	0.27
9	Ultrafilter	965	0.34
10	Nanofilter	413	0.21
11	Nanofilter	413	0.27
12	Nanofilter	413	0.34
13	Nanofilter	689	0.21
14	Nanofilter	689	0.27
15	Nanofilter	689	0.34
16	Nanofilter	965	0.21
17	Nanofilter	965	0.27
18	Nanofilter	965	0.34
19	Nanofilter	1206	0.21
20	Nanofilter	1206	0.27

each batch run from room temperature to around 40°C, so that flow rates were adjusted to flux at 25°C. Feed and concentrate samples were taken and measured for pH, oil content, and conductivity. COD was measured using the standard Hach test method (8). Oil percentages of the feed and concentrate samples were analyzed with the acid-split test, in which sulfuric acid was added to split the emulsion and the floating oil layer measured in a graduated cylinder. From the data obtained, flux characteristics and permeate quality were compared.

Test Program

In the coolant test program, the effects of varying both pressure and feed flow were analyzed using the ultrafilter and nanofilter. Table 1 lists all the runs. In each run, the same virgin coolant solution was processed; a solution was made from coolant concentrate that contained 15% oil by volume as analyzed by the acid split test. The permeate was collected from each run and used to flush the system as a cleaning step prior to the following run.

Marcel Dekker, Inc.
270 Madison Avenue, New York, New York 10016

RESULTS AND DISCUSSION

In order to control as many variables as possible, the same solutions were used repeatedly. Even though each type of oily solution contained many different types of solutes (oil, surfactants, salts, other organics), the initial concentration was maintained constant for each run. Figures 2a and 2b depict the flux behavior for typical coolant runs at 413 kPa average transmembrane pressure. For the sake of brevity, complete runs are presented only for operating pressures at 413 kPa. Average initial flux values for each run can be found in the third column of Tables 2 and 3. In all concentration runs, the same trends were observed: As the solution was concentrated, flux declined steadily and permeate quality worsened. The permeate samples at low recovery appeared cleaner; as the solutions were concentrated, the permeate became darker in color. For the most part, the test runs were allowed to continue and permeate samples taken until the flux dropped to below 3 liters/m^2/hr (LMH). The following discussion develops both quantitative and qualitative interpretations of the results obtained.

Flux Behavior—Mass Transfer Model

Based on a comparison of three applicable models (mass transfer, resistance, osmotic), the mass transfer model provided the best fit. Though the resis-

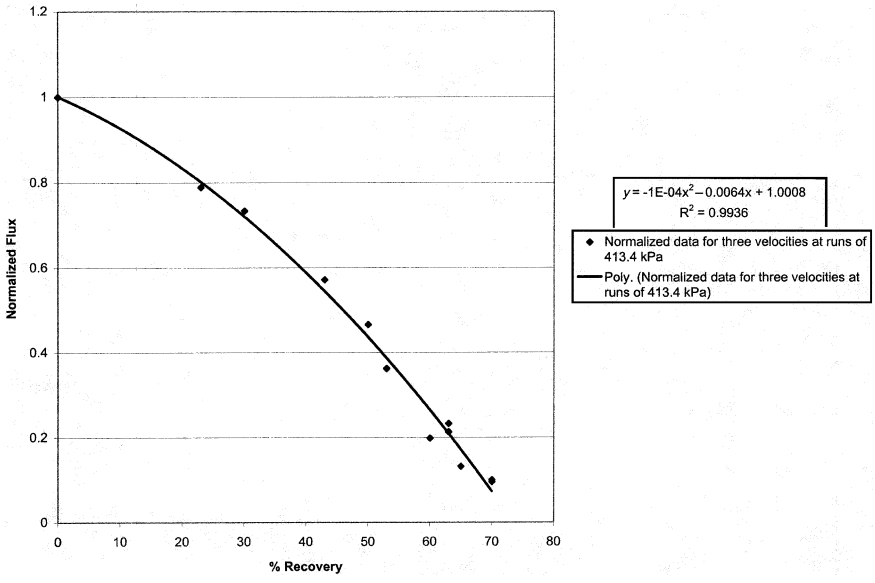

Figure 2a. Normalized UF flux for machining coolant.

MARCEL DEKKER, INC.
270 Madison Avenue, New York, New York 10016

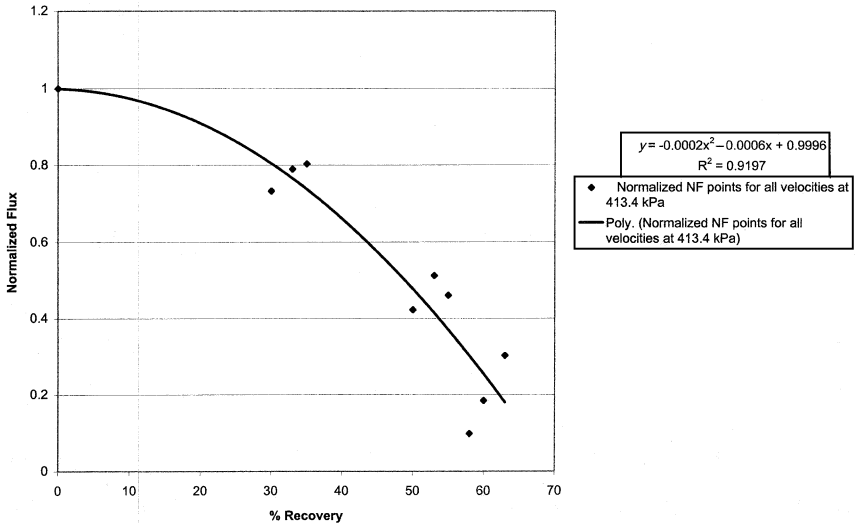

Figure 2b. Normalized NF flux for machining coolant.

tance model is easier to apply in the pressure-dependent region, the mass transfer model is applicable to any applied pressure situation. Convective transport of solute to the membrane surface occurs in both the pressure-dependent and independent regions, thus resulting in the formation of a gel layer and subsequent back diffusion. While the results (presented later) may indicate that a pressure-dependent model could be appropriate for the nanofiltration runs, the mass transfer model was used to set up a comparative analysis of nanofiltration versus ultrafiltration.

Table 2. Mass Transfer Coefficient Determination of Ultrafiltration Coolant Runs

Run #	Press., Vel.	Ave. Initial Flux, (LMH)	*k*, (LMH)	*R*, Correl. Factor	# Samples
1	413 kpa, 0.21 m/sec	15.5	11.6	0.989	5
2	413 kpa, 0.27 m/sec	16.6	12.0	0.989	5
3	413 kpa, 0.34 m/sec	17.0	12.2	0.992	5
4	689 kpa, 0.21 m/sec	10.4	7.5	0.984	5
5	689 kpa, 0.27 m/sec	13.4	9.2	0.987	5
6	689 kpa, 0.34 m/sec	13.8	9.4	0.962	5
7	965 kpa, 0.21 m/sec	11.5	9.0	0.993	5
8	965 kpa, 0.27 m/sec	12.7	9.3	0.996	5
9	965 kpa, 0.34 m/sec	13.6	9.5	0.995	5

Table 3. Mass Transfer Coefficient Determination of Nanofiltration Coolant Runs

Run #	Press., Vel.	Ave. Initial Flux, (LMH)	*k*, LMH	*R*, Correl. Factor	# Samples
10	413 kPa, 0.21 m/s	12.1	9.2	0.962	5
11	413 kPa, 0.27 m/s	12.9	9.8	0.975	5
12	413 kPa, 0.34 m/s	14.6	10.8	0.993	5
13	684 psi, 0.21 m/s	13.9	10.3	0.939	5
14	684 psi, 0.27 m/s	16.0	10.8	0.996	5
15	684 psi, 0.34 m/s	19.2	14.7	0.975	5
16	965 psi, 0.21 m/s	18.7	13.0	0.939	5
17	965 psi, 0.27 m/s	20.4	14.9	0.996	5
18	965 psi, 0.34 m/s	26.2	18.2	0.975	5
19	965 psi, 0.21 m/s	19.0	13.8	0.947	5
20	965 psi, 0.27 m/s	20.0	14.2	0.968	5

In the mass transfer model, the existence of the solute concentration gradient is used to help predict flux behavior. Equation (1) is used to determine k, the mass transfer coefficient. A constant C_m value is assumed and used in all calculations based on experimental results and published literature. When ΔP is high enough, the concentration at the membrane surface can be written as C_g, the gel layer concentration. Since the mass transfer model (Eq. 1) states that the flux becomes zero when the bulk concentration C_b, is equal to C_g, results obtained in this study can also be used to determine C_g. The maximum attainable oil concentration in oil-in-water emulsions is about 60% v/v (9). Oil emulsion droplets can be viewed as micron-size colloids that are in a close-packed arrangement in the gel layer. Acid split tests on end concentrate samples indicate oil concentrations of around 55%. As seen in Figs. 2a and 2b, the flux curves tend toward 70–75% recovery at zero flux. The concentration of a solute C at any point in the concentration cycle can be computed as follows:

$$C_{(\%\ \text{recovery})} = C_i/(1 - \%\ \text{recovery}) \tag{4}$$

where $C_{(\%\ \text{recovery})}$ is the concentration of solute at a particular % recovery and C_i is the initial solute concentration (at 0% recovery). The oil concentration at 75% recovery is 60%, as calculated with Eq. (4).

$C_g = 0.60$ is a reasonable value since the end concentrate samples were taken when fluxes dropped to approximately 3 LMH, and the measured concentration of 0.55 would be slightly lower than the true maximum oil concentration. In the mass transfer model, C_g is also assumed to be constant; C_g is only a function of the solute-solvent system and temperature, but it is independent of the membrane characteristics, feed concentration, flow conditions, and operating pressure (10). Therefore, the same C_g estimate of 0.60 is used in all calculations.

UF Mass Transfer Coefficient Determination

Plots of flux vs. $\ln(C_m/C_b)$ were generated using the UF experimental results, Eq. (4), and the constant $C_m = C_g = 0.60$. Equation (4) is valid if 100% of the solute (oil) is rejected. Since only truly soluble oil in water can permeate the membrane and the mineral oil solubility in water is very low, the solute concentration difference across the membrane is essentially the feed concentration. Oil and grease test results on selected permeate samples were all below 100 mg/l or 0.01%. Therefore, 100% oil separation of a solution with >15% oil is a good assumption. From the plots, the mass transfer coefficients for each individual run can be calculated. Figure 3a depicts the linear relationship between the flux (J) and $\ln(C_m/C_b)$ for each run at 413 kPa. From Eq. (1), k can be calculated as the slope of these straight lines.

As mentioned earlier, k is the diffusivity of the solute per boundary layer thickness in the solvent, which is water. Facilitating the back-transport of solute away from the membrane surface would increase flux. If the Reynolds number is increased, the mass boundary layer thickness is reduced and the mass transfer coefficient increases. The model indicates that k will increase with the feed velocity, v (Eq. 3). This effect can be seen in Fig. 3a where increasing the tangential velocity steepens the lines (i.e., increases slopes) and thus raises the values of k. While some scatter of data is evident, a trend is observed.

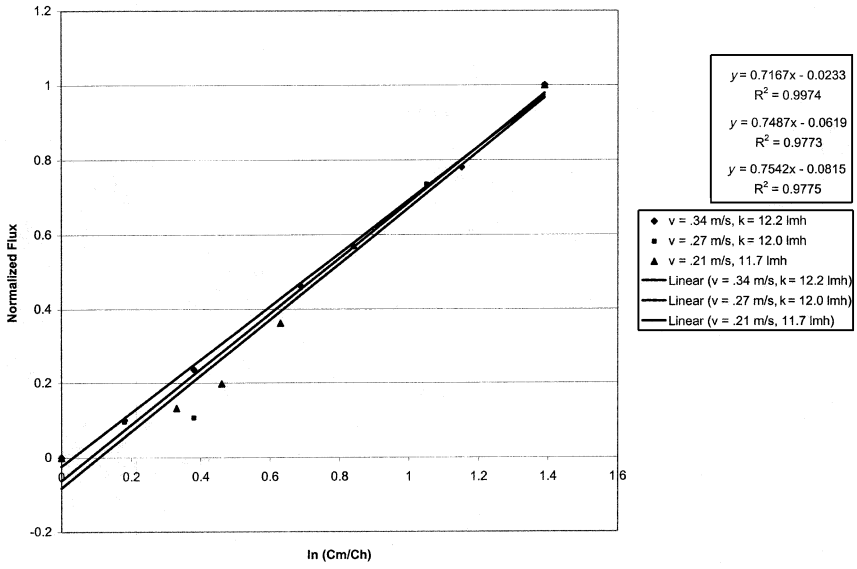

Figure 3a. Normalized UF mass transfer coefficient determination at 413 kPa.

MARCEL DEKKER, INC.
270 Madison Avenue, New York, New York 10016

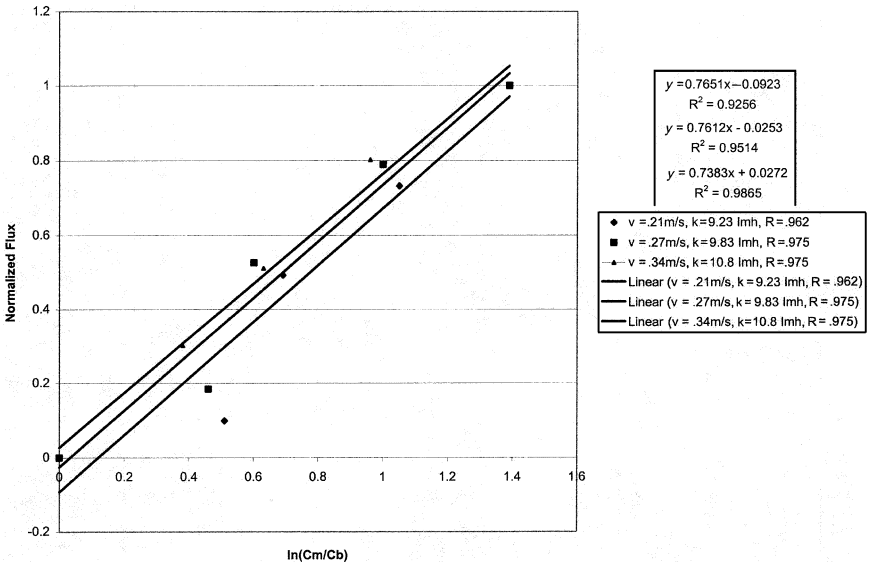

Figure 3b. Normalized NF mass transfer coefficient determination at 413 kPa.

Table 2 summarizes the results of each run from 413 kPa to 965 kPa. As predicted by theory, increasing the feed (tangential) velocity increases k and permeate flux. However, increasing P above 413 kPa affects the permeate flux *negatively*. As a result, k *decreases* with increasing pressure. More discussion of this phenomenon is presented later.

NF Mass Transfer Coefficient Determination

The same assumptions used in the mass transfer coefficient determination for the ultrafiltration runs are used in the determination of the nanofiltration mass transfer coefficients. The results can be found in Table 3 and plots for 413 kPa runs seen in Fig. 3b. Similar to the UF runs, increasing the feed velocity has a positive effect on k. Unlike the UF runs, however, increasing the transmembrane pressure also increases k.

While good correlations are also observed in this set of analyses, one potential major factor may be neglected. In the UF analysis, it is assumed that oil is the only rejected solute since the pore size of the UF membrane is relatively large (15,000 molecular weight cutoff). Since the NF membrane has much smaller pores (500 molecular weight cutoff) and is capable of partial ion rejection, other rejected solute constituents can exist and become part of the gel layer. The method used to determine k is based on the assumption that oil is the predominant solute.

Because the machining coolant contains a relatively low amount of total dissolved solids (TDS) compared with other solutions such as washwater, it may be valid to assume that oil is the major solute species. Other tests on washwater with high TDS levels have demonstrated significant osmotic effects; the coolant samples in this study did not. Since final percent recoveries are similar in the UF and NF runs (60 to 70%), it is reasonable to believe that oil is the predominant solute that limits flux in both membrane processes. Equation (1) is satisfied in both cases. Only when the solution becomes highly concentrated (high % recovery) in the nanofiltration runs may other mass transfer activities be more significant.

The gel layer becomes more significant at higher operating pressures because of increased convective transport of solute to the membrane surface. In addition, too much applied pressure can result in further compaction or densification of the gel layer against the membrane surface, which then increases resistance further and reduces flux (6). Also, because the UF membrane has larger pores, some surface pore blockage may also be occurring. Any surface pore blockage will reduce flux. Figures 4a and 4b, and the third column in Tables 2 and 3, demonstrate the effect of increasing the applied transmembrane pressure on flux at 0% recovery. In the ultrafiltration runs, flux *declines* as more pressure is applied because of this gel layer compaction and pore blockage phenomenon. In the same pressure range for the nanofiltration runs, however, flux *increase* is observed.

As mentioned above, the nanofiltration boundary and gel layers are chemically different from those of ultrafiltration. Other studies performed by the authors have demonstrated that because nanofiltration is more sensitive to osmotic

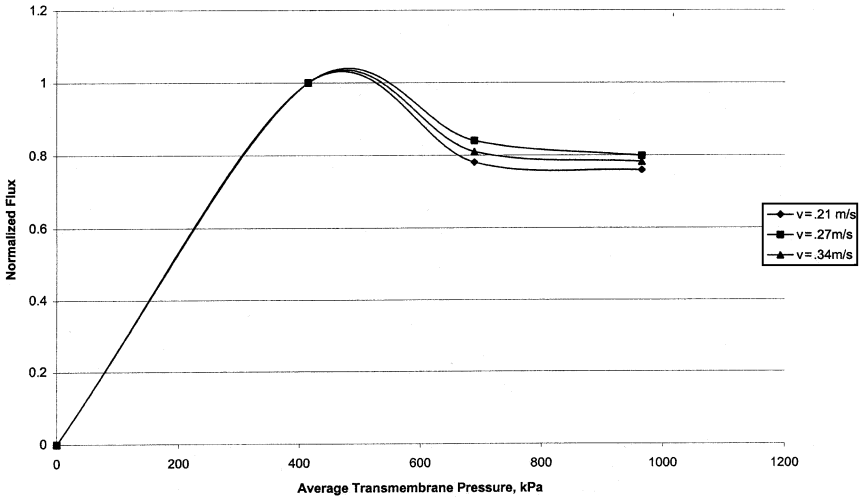

Figure 4a. Normalized UF flux vs. pressure.

MARCEL DEKKER, INC.
270 Madison Avenue, New York, New York 10016

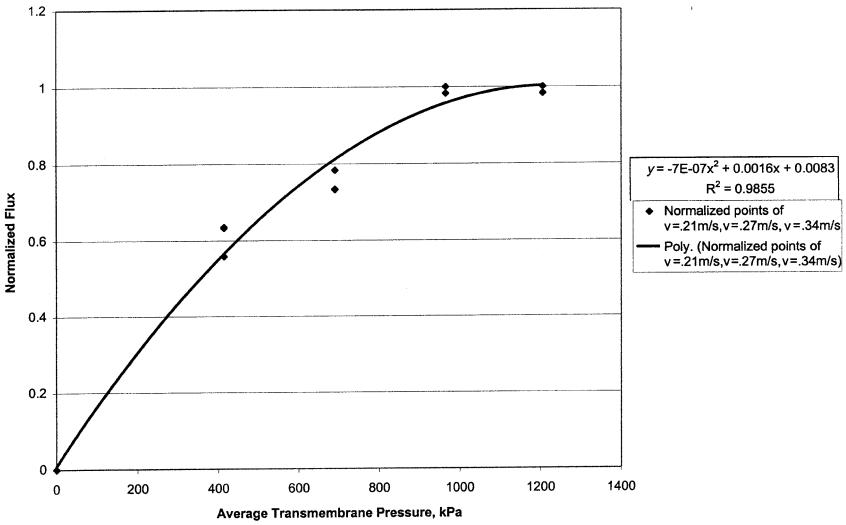

Figure 4b. Normalized NF flux vs. pressure.

pressure, other solutions that exhibit high levels of total dissolved solids will not separate as efficiently as the coolant tested in this project. The added presence of salts and other organics in the NF gel layer may affect the compressibility of the gel material such that increasing ΔP does not densify the gel layer as observed in the UF runs. In addition, since the NF membrane pores are much smaller than those of the UF membrane, surface pore blockage is less likely at higher pressures. As a result, increasing pressure from 413 kPa results in a positive increase in NF flux.

An alternate mechanism by Bowen et al. (11,12) suggests that the critical pressure is applied when hydrodynamic forces, transporting the colloid or particles toward the membrane pore, are balanced by an opposing electrostatic force created as the colloid approaches the membrane or gel surface. Because our critical pressure appears to be a function of the pore-size, this alternate mechanism is not appropriate.

Permeate Quality Comparison

Visually, the coolant ultrafiltration permeate is clear but exhibits a yellowish color. The nanofiltration permeate is clear with almost no color; the chemicals that incur color are low molecular weight species that are rejected by the nanofilter. In both UF and NF runs, the permeate becomes darker in color as the solution is concentrated. Figures 5a and 5b display the COD and conductivity levels in the

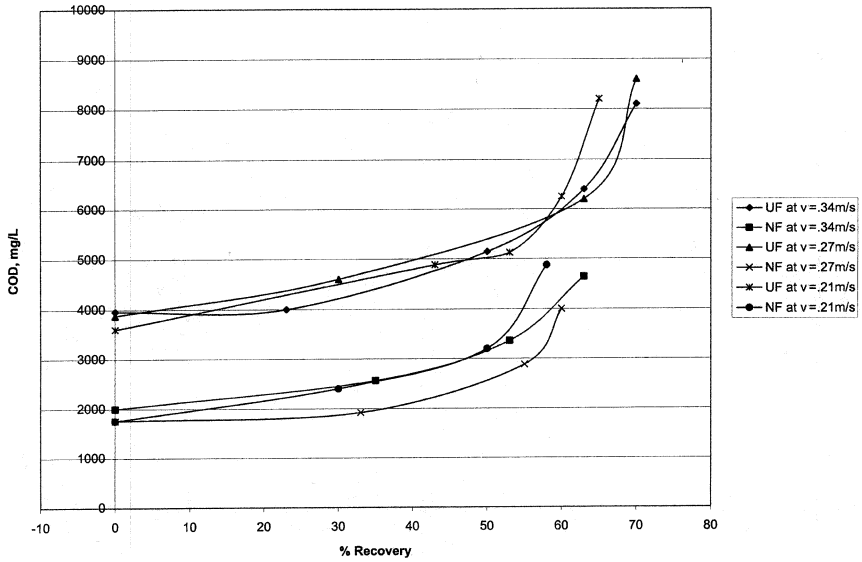

Figure 5a. COD results, UF and NF runs at 413.4 kPa.

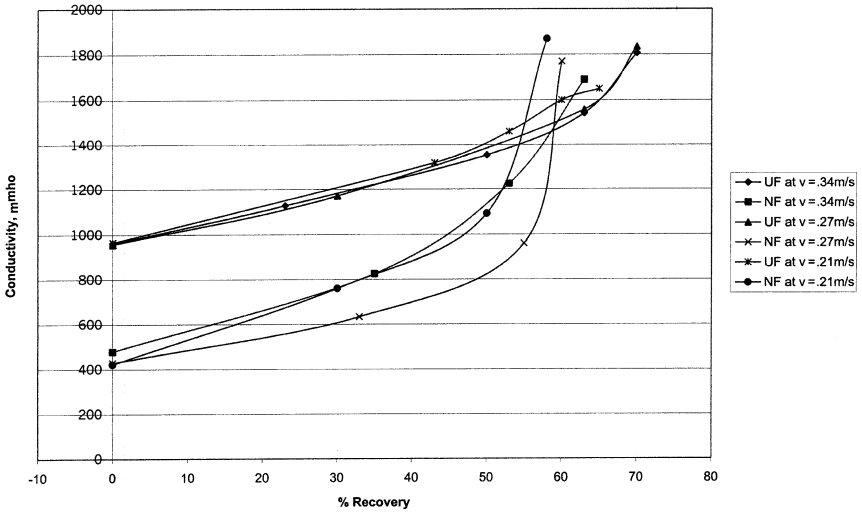

Figure 5b. Conductivity results, UF and NF runs at 413.4 kPa.

MARCEL DEKKER, INC.
270 Madison Avenue, New York, New York 10016

965 kPa coolant runs. Except for at high % recoveries, the data indicate the NF permeate to contain lower levels of COD and dissolved solids. The pH of all of the raw and permeate coolant samples is 9.0.

Where similar end % recoveries are achieved, the quality of the NF permeate resembles that of the UF permeate at high % recoveries (see Figs. 5a and 5b). This may lead one to believe that "leakage" of the nanofiltration membrane is occurring. However, since the NF membrane rejects many more constituents than the UF membrane, the concentrate contains higher levels of these rejected materials. Since membranes are not 100% rejecting due to a distribution of pore sizes, permeate solute concentration is strongly dependent on the feed solute concentration. If a particular membrane is rated for a 90% separating efficiency for solute *X* and the feed contains 1000 mg/l of solute *X*, then the permeate should have 100 mg/l of solute *X*. If the feed contains 10,000 mg/l of solute *X*, the permeate will hold 1,000 mg/l. As seen in Figs. 5a and 5b, permeate quality worsens as the solution is concentrated. The separating efficiency of the NF membrane has not changed; instead, the NF concentrate has become more complex with high concentrations of those organics and salts that are relatively low in concentration at the beginning of the runs. The result is that NF permeate is no longer cleaner than UF permeate at very high feed concentrations.

Economic Comparison

In these coolant runs, the energy requirement for the nanofiltration process is comparable to those for ultrafiltration. In fact, at higher pressures, the NF process appears to be more efficient. As discussed earlier, increasing operating pressure (thereby increasing energy costs) results in a decrease in UF flux, most likely due to gel compaction and surface pore blockage. The most efficient range for the ultrafiltration process is at relatively low pressures; slightly higher operating pressures will provide higher nanofiltration flux processes (see Figs. 4a and 4b).

CONCLUSION

For the particular coolant tested in this study, it appears that nanofiltration can provide better separation than ultrafiltration without sacrificing flux and % recovery. Only at very high % recoveries are the permeate qualities similar; a process designed to operate in a batch mode can provide for better overall permeate quality. Because oily wastewater is very common and broad-based, pilot testing is required to determine the feasibility of utilizing nanofiltration for each oily waste stream.

MARCEL DEKKER, INC.
270 Madison Avenue, New York, New York 10016

REFERENCES

1. Cadotte, J.; Forester, R.; Kim, M.; Petersen, R.; Stocker, T. Nanofiltration Membranes Broaden the Use of Membrane Separation Technology. Desalination **1988**, *70*, 77–88.
2. Desalination Systems Inc. Product Bulletin on DS-5 membrane.
3. Desalination Systems Inc. Product Bulletin on G-50 membrane.
4. van den Berg, G. B.; Smolders, C.A. *Flux Decline in Membrane Processes*, presented to the Filtration Society, London, November 1987.
5. Cheryan, M. Ultrafiltration Handbook; Technomic Publishing Company: Lancaster, PA 1986.
6. Schweitzer, P. A. *Handbook of Separation Techniques for Chemical Engineers*; McGraw-Hill: New York, 1979.
7. Perry, R. H.; Green, D. Perry's Chemical Engineer's Handbook, 6th Edition; McGraw-Hill: New York, 1984.
8. Clesceri, L. S.; Greenby, A. E.; Trussel, R. R. Standard Methods for the Examination of Water and Wastewater, 17th Edition; American Public Health Association: Washington, 1989.
9. Pinto, S. *Ultrafiltration for Dewatering of Waste Emulsified Oils*. Lubrication Challenges in Metalworking and Processing, Proceedings 1st International Conference, Chicago, 1978.
10. Ho, W.; Sirkar, K. *Membrane Handbook*; Van Nostrand Reinhold: New York, 1992.
11. Bowen, W. R.; Hillal, N.; Jain, M.; Lovitt, R. W.; Sharif, A. O.; Wright, C. J. The Effects of Electrostatic Intersections on the Rejection of Colloidal by Membrane Pores. Chemical Engineering Science **1999**, *54*, 369–375.
12. Bowen, W. R.; Sharit, A. O. Hydrodynamic and Colloidal Interactions. Chem. Eng. Sci. **1998**, *53,* 879–890.

Received December 1999
Revised September 2000

Request Permission or Order Reprints Instantly!